Clicked $(AB)_2C$-Type Miktoarm Terpolymers: Synthesis, Thermal and Self-Assembly Properties, and Preparation of Nanoporous Materials

Jie Song,[1] Eunji Lee,[2] Byoung-Ki Cho[1]
[1]Institute of Nanosensor and Biotechnology, Department of Chemistry, Dankook University, Gyeonggi-Do 448-701, Korea
[2]Graduate School of Analytical Science and Technology, Chungnam National University, Daejon 305-764, Korea
Correspondence to: E. Lee (E-mail: eunjilee@cnu.ac.kr) or B.-K. Cho (E-mail: chobk@dankook.ac.kr)

Received 13 August 2012; accepted 2 October 2012; published online 29 October 2012
DOI: 10.1002/pola.26403

ABSTRACT: A well-defined (PEO-PS)$_2$-PLA miktoarm terpolymer (**1**) was synthesized by stepwise click reactions of individually prepared poly(ethylene oxide) (PEO), polystyrene (PS, polymerized by atom transfer radical polymerization), and polylactide (PLA, polymerized by ring-opening polymerization) blocks. As characterized by differential scanning calorimetry and small-angle X-ray scattering techniques, the terpolymer self-assembled into a hexagonal columnar structure consisting of PLA/PEO cylindrical cores surrounded by PS chains. In contrast, the ion-doped sample (**1-Li**$^+$) with lithium concentration per ethylene oxide $= 0.2$ exhibited a three-phase lamellar structure, which was attributed to the microphase separation between PEO and PLA blocks and to the conformational stabilization of the longest PLA chain. The two-phase columnar morphology before the ion doping was used to prepare a nanoporous material. PLA chains in the cylindrical core region were hydrolyzed by sodium hydroxide, producing nanopores with a pore diameter of about 14 nm. The resulted nanoporous material sank to the bottom in water, because of water-compatible PEO chains on the walls. © 2012 Wiley Periodicals, Inc. J Polym Sci Part A: Polym Chem 51: 446–456, 2013

KEYWORDS: block copolymers; click chemistry; miktoarm polymers; phase separation; self-assembly

INTRODUCTION Alteration of polymeric architecture has a significant influence on many physical natures of polymers, for example, solution, thermal, and self-assembling properties.[1] Thus, the topological control of polymeric materials is an important parameter to engineer polymer properties, and many efforts have been made to prepare macromolecules with new polymeric architectures.

Indeed, branched polymers encompassing random hyperbranched polymers, dendrimers, and star polymers have been widely studied and applied on coatings, additives, and supramolecular building blocks. Recently, asymmetric dendritic-linear or miktoarm block copolymers have been reported as a new class of branched macromolecules,[2] which consist of multiple polymeric blocks of different size and chemical identity. These hybrid types are of great interest particularly in bulk and solution assembling properties. For example, several studies in the bulk assembling of dendritic-linear block copolymers demonstrated that the hybrid system could share the morphological properties of self-assembling dendritic polymers and linear block copolymers.[3] In addition to the bulk assemblies, miktoarm star polymers bearing distinct polymeric arms have shown dynamic morphological changes (e.g., micelle to unimer transition under certain conditions) because the constituting polymeric components could be designed to be individually responsive to external stimuli such as pH, temperature, light, and solvent.[4] Such morphological diversity is versatile as a model of delivery vehicle, which is practically important.

For this reason, it is worth the challenge of building more complex polymeric architectures to explore new polymer functions. Indeed, many polymerization and coupling methods have been combined to construct complex miktoarm star and dendritic polymers. For example, the Percec group devised a divergent synthetic method consisting of living radical polymerization and AB$_2$-type terminator multifunctional initiator (TERMINI) for the preparation of complex dendritic polymers with polymeric poly(methyl methacrylate) spacers. A focal group (A) of the TERMINI molecule terminates the living polymer by coupling with the polymer end, and two demasked groups (B) reinitiate a living polymerization with 100% efficiency. By this reason, in contrast to hyperbranched polymers, the dendritic polymers from the TERMINI method have flawless chain structures with narrow molecular weight distributions.[5] Among many coupling methods, “click reactions” such as copper(I)-catalyzed cycloaddition, thio-bromo coupling, and Diels-Alder coupling have received much attention because of their synthetic merits such as high reactivity, free of protection, and simple workups.[6] Nowadays, this click coupling has enabled more complicated molecular/polymeric assembling systems, including liquid crystals, dendrimers, and block codendrimers, to be designed and synthesized.[6(b–e),7]

With this in mind, we envisioned that complex miktoarm polymers could be prepared by a combination of controlled polymerizations and click chemistry. To date, various architectured miktoarm polymers such as AB_2, ABC, ABCD, A_2B_2C, and A_7B_7 have been reported;[8] however, in most cases, the polymer individuals connected to a core group have been homopolymers. On the other hand, diblock copolymers rather than homopolymers can be connected to the core as a polymer component, by which more complex miktoarm polymers can be produced. The complicated structures may be accomplished more readily by means of the efficient click chemistry. Thus, we designed and synthesized a $(AB)_2C$-type miktoarm terpolymer in which A, B, and C are poly(ethylene oxide) (PEO), polystyrene (PS), and polylactide (PLA), respectively. The synthetic strategy in this work involved stepwise click reactions of the individually prepared polymeric units. Before click reactions, well-defined PS and PLA polymer units could be prepared by atom transfer radical polymerization (ATRP) and ring-opening polymerization (ROP), respectively.

In addition to the synthesis issue, we were interested in the bulk assembling behavior of the new terpolymer. Considering the miscibility between the blocks in the miktoarm terpolymer, the PLA and PEO chains might be mixed with each other unless a PEO crystallization occurs,[9] thus forming a single domain at the molecular level. On the other hand, it is known that PEO blocks become more polar on a selective complexation with ionic species such as lithium salts, which sometimes segregates PEO blocks from other polymeric blocks in the bulk state.[10] Therefore, we envisaged that an ion doping of the PEO part of the terpolymer could be microphase separated from the others, which might induce a different morphology in which the three blocks are segregated.

Finally, we attempted to prepare nanoporous materials because the terpolymer contained mechanically robust PS and degradable PLA blocks.[11] According to morphology interpretations, we could use a two-phase columnar morphology in which the PEO and PLA blocks are located in a confined space, and a nanoporous structure could be expected by etching the PLA block in the ordered morphology. In this article, we reported all the details regarding the above results.

EXPERIMENTAL

Materials

4-Pentynoic acid (95%), propargyl amine (98%), 2-bromoisobutyryl bromide (98%), 3,5-dihydroxybenzyl alcohol (99%), propargyl bromide solution (80 wt % in toluene), 4-(dimethylamino)pyridine (DMAP, 99%), sodium azide (>99.99%), methanolic HCl (1.25 M in methanol), triethyl aluminum (1.0 M solution in hexanes), copper(I) bromide (99.999%), *N,N,N′,N″,N″*-pentamethyldiethylenetriamine (PMDETA, 99%), copper(II) sulfate pentahydrate ($CuSO_4{\cdot}5H_2O$, 99.999%), and (+)-sodium L-ascorbate (≥98%) were purchased from Sigma-Aldrich Chemical. D,L-Lactide (Aldrich) was purified by recrystallization from toluene and then dried under reduced pressure at room temperature. All other chemicals were purchased from commercial sources and used as received without further purification. Styrene (≥99%, Aldrich) was dried by stirring over CaH_2 (Acros) for 24 h and distilled under reduced pressure. α-Methoxy-ω-azide-poly(ethylene glycol) (**PEO-N$_3$**) was synthesized by following a procedure described previously.[12] The ROP of D,L-lactide was performed using an azido-alcohol initiator, as described previously.[13] The ion-doped terpolymer (**1-Li$^+$**) was prepared by mixing the terpolymer (**1**) solution in dry tetrahydrofuran (THF) with an appropriate volume of 0.1 mmol/mL lithium triflate in dry THF, followed by slow evaporation of the solvent under reduced pressure. The samples were then dried in a vacuum oven to maintain constant mass.

Methods

^1H and ^{13}C NMR spectra were recorded at room temperature on Varian 200 and Varian 500 spectrometers, using chloroform-*d* ($CDCl_3$) as the solvent and tetramethylsilane as the internal reference for chemical shifts. Gel permeation chromatography (GPC) measurements were performed on a waters system equipped with a Waters 510 HPLC pump, a Waters M486 tunable absorbance detector, a Waters M410 differential refractive index detector, and three Waters Styragel HR columns with a continuous porosity of 10^2–10^4 Å. THF (with 2% *N,N*-dimethylacetamide) was used as the mobile phase, and the rate was 1.0 mL/min at 35 °C. Matrix-assisted laser desorption ionization time-of-flight (MALDI-TOF) mass spectra were obtained on a Perceptive Biosystems Voyager-DE STR system equipped with a 337-nm nitrogen laser, using dithranol as the matrix. Mass spectra were acquired in reflector mode at an acceleration voltage of +20 kV. Differential scanning calorimetry (DSC) analyses were performed on a Perkin-Elmer DSC-7 instrument. Indium and zinc standards were used for temperature and enthalpy calibrations, and nitrogen (10 mL/min) was used as the purge gas. The scan rate used for the samples was 10 °C/min. Small-angle X-ray scattering (SAXS) measurements were performed in transmission mode with synchrotron radiation at the 10C1 X-ray beam line (Pohang Accelerator Laboratory, Korea). Scanning electron microscopic (SEM) samples were analyzed with a Hitachi S-4300 FE-SEM, using an acceleration voltage of 15 kV. The secondary electron images were collected in ultrahigh resolution mode at a working distance of ∼ 5 mm. The platinum coating thickness was about 2 nm, which was estimated from a calculated deposition rate and an experimental deposition time. The macroscopic alignments were performed with a home-built channel die 3 mm wide and 60 mm long. Hot-pressed pieces of polymer samples were placed in the center of the channel die and then heated to 130 °C in a laboratory press. The samples were subjected to compression with a constant load (compression

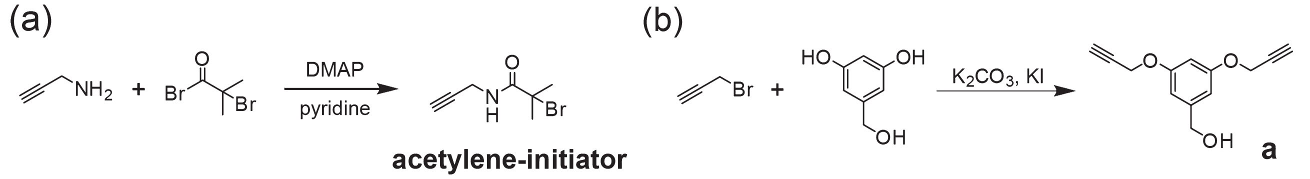

SCHEME 1 Synthetic routes of (a) ATRP initiator containing acetylene unit and (b) branching precursor (**a**) bearing two acetylene units.

ratio ~ 10) and allowed to cool to room temperature over a period of 1 h before removing them from the channel die. The thicknesses of aligned samples were between 0.5 and 1 mm.

Synthesis

The general synthetic procedures are outlined in Schemes 1 and 2.

2-Bromo-2-methyl-N-(prop-2-ynyl)propanamide (Acetylene-Initiator)

Propargyl amine (1.5 g, 27.2 mmol, 1.0 equiv), DMAP (3.33 g, 27.2 mmol, 1.0 equiv), and pyridine (10.8 g, 136.2 mmol, 5.0 equiv) were dissolved in 50 mL of anhydrous THF at 0 °C, and a solution of 2-bromoisobutyryl bromide (7.52 g, 32.7 mmol, 1.2 equiv) in anhydrous THF (20 mL) was slowly added under stirring. The reaction mixture was stirred in the cooling bath for 1 h and then at room temperature for another 6 h. The remaining acid bromide was quenched by adding methanol (7 mL) and stirred for 15 min. After insoluble solid was filtered off, the solvent was removed using a rotary evaporator. The residue was redissolved in CH_2Cl_2 and then treated with diluted aqueous HCl solution. The organic layer was washed thrice with brine. After removing the solvent, the crude product was purified by silica column chromatography (from *n*-hexane: CH_2Cl_2 = 7:3 to CH_2Cl_2) to give **acetylene-initiator** (3.5 g, 63%) as a white solid. TLC (eluent; CH_2Cl_2): R_f 0.73.

^1H NMR ($CDCl_3$): δ 6.91 (br, 1H, CH≡CCH$_2$N**H**CO), 4.06 (m, 2H, CH≡CC**H**$_2$NHCO), 2.28 (t, 1H, C**H**≡CCH$_2$NHCO), 1.96 [s, 6H, NHCO(C**H**$_3$)$_2$Br]. ^{13}C NMR ($CDCl_3$): δ 172.2, 79.4, 72.7, 62.8, 33.1, 30.9.

(3,5-Bis(prop-2-ynyloxy)phenyl)methanol (a)

3,5-Dihydroxybenzyl alcohol (2.0 g, 14.3 mmol, 1.0 equiv), K_2CO_3 (6.0 g, 42.8 mmol, 3.0 equiv), and KI (2.37 g, 14.3 mmol, 1.0 equiv) were dissolved in 70 mL of anhydrous acetonitrile. Then, a solution of propargyl bromide (80 wt % in toluene, 4.25 g, 35.7 mmol, 2.5 equiv) was added. The reaction mixture was stirred at 85 °C for 24 h under nitrogen. After insoluble solid was filtered off, the solvent was removed using a rotary evaporator. The residue was redissolved in CH_2Cl_2 and treated with diluted aqueous HCl solution. The organic layer was washed thrice with brine. After evaporating the solvent, the crude product was purified by silica column chromatography (from CH_2Cl_2:EtOAc = 49:1 to 4:1) to give compound **a** (2.1 g, 69%) as a white solid. TLC (eluent; CH_2Cl_2:EtOAc = 19:1): R_f 0.57.

^1H NMR ($CDCl_3$): δ 6.63 (d, 2H, Ar-**H**), 6.54 (t, 1H, Ar-**H**), 4.67 (d, 4H, CH≡CC**H**$_2$O-Ar), 4.63 (s, 2H, Ar-C**H**$_2$OH), 2.52 (t, 2H, C**H**≡CCH$_2$O-Ar), 1.73 (t, 1H, Ar-CH$_2$O**H**). ^{13}C NMR ($CDCl_3$): δ 159.3, 144.1, 106.8, 102.1, 78.9, 76.2, 65.7, 56.5.

Acetylene-PS-Br

The PS was prepared by the ATRP of styrene using the compound **acetylene-initiator** as the initiator and Cu(I)Br/

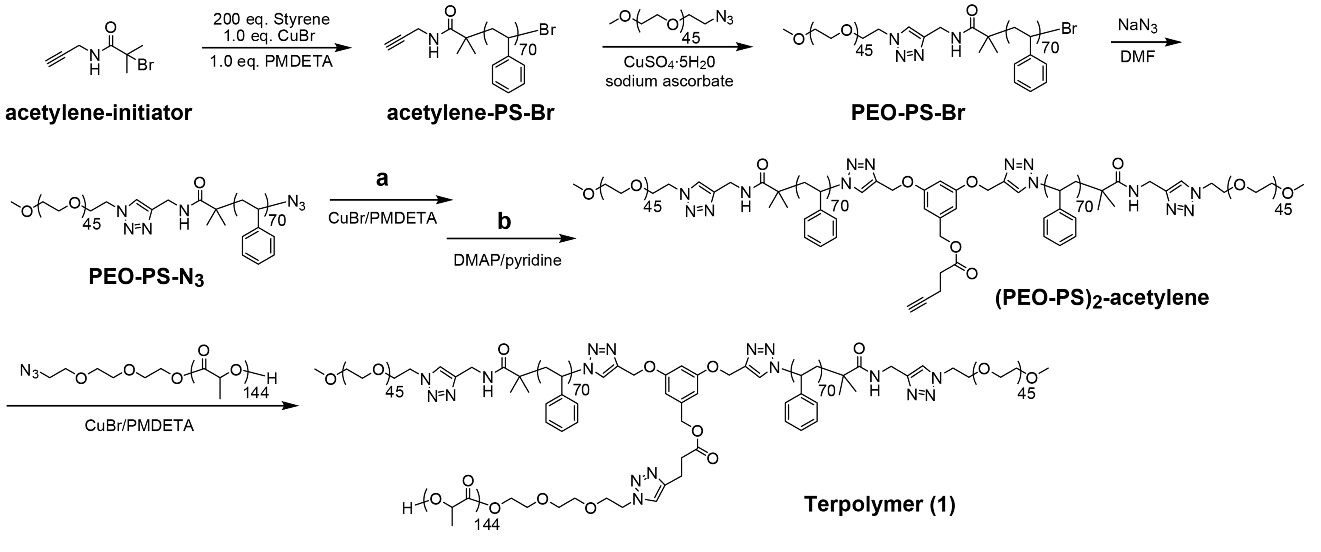

SCHEME 2 Synthesis of (PEO-PS)$_2$-PLA terpolymer (**1**) using stepwise click reactions.

PMDETA as the catalyst. In a glove box, **acetylene-initiator** (421.2 mg, 2.064 mmol, 1.0 equiv), Cu(I)Br (296.1 mg, 2.064 mmol, 1.0 equiv), deoxygenated PMDETA (357.7 mg, 2.064 mmol, 1.0 equiv), and deoxygenated styrene (43 g, 412 mmol, 200 equiv) were added into a 60 mL of Schlenk tube. The reaction mixture was stirred for 10 min at room temperature. The tube was then placed in an oil bath thermostated at 90 °C for 1 h. The polymerization reaction was quenched by dipping the tube in liquid nitrogen. The mixture was then diluted with THF and passed through a neutral alumina column to remove the copper catalyst. After evaporation of the solvent, the resulting polymer was purified thrice by dissolution/precipitation with THF/cold methanol. The obtained polymer was dried at 40 °C in a vacuum oven for 12 h to give the PS product (5.0 g) as a white solid. $M_{n(GPC)} = 7800$ g/mol; $M_w/M_{n(GPC)} = 1.04$. $M_{n(NMR)} = 7500$ g/mol.

^1H NMR (500 MHz, $CDCl_3$): δ 7.26–6.27 (aromatic protons, repeating unit of PS), 5.32–5.16 ($CH{\equiv}CCH_2N\mathbf{H}CO$), 4.61–4.33 [$CH_2C\mathbf{H}$(Ph)-Br, end group of PS], 3.78–3.43 ($CH{\equiv}CC\mathbf{H}_2NHCO$), 2.58–1.16 [$C\mathbf{H}_2C\mathbf{H}$(Ph), repeating unit of PS backbone], 1.08–0.78 [NHCOC($C\mathbf{H}_3$)$_2$].

PEO-PS-Br

α-Methoxy-ω-azide-poly(ethylene glycol) [**PEO-N$_3$**, $M_{n(NMR)} = 2000$ g/mol, 0.57 g, 0.285 mmol, 1.0 equiv], **acetylene-PS-Br** [$M_{n(NMR)} = 7500$ g/mol, 2.35 g, 0.314 mmol, 1.1 equiv], $CuSO_4{\cdot}5H_2O$ (71.2 mg, 0.285 mmol, 1.0 equiv), and sodium ascorbate (170 mg, 0.855 mmol, 3.0 equiv) were dissolved in CH_2Cl_2 (14 mL) and H_2O (7 mL). The reaction mixture was stirred for 2 h at room temperature and then diluted with CH_2Cl_2 and H_2O. The organic layer was washed thrice with brine. After removal of the organic solvent, the crude product was purified by flash silica-column chromatography (from CH_2Cl_2:EtOAc = 9:1 to CH_2Cl_2:methanol = 8:1). The resulting polymer was dried at 30 °C in a vacuum oven for 20 h to give **PEO-PS-Br** (1.55 g, 58%) as a white solid. $M_w/M_{n(GPC)} = 1.03$.

^1H NMR (500 MHz, $CDCl_3$): δ 7.56–7.40 (proton in triazole), 7.26–6.27 (aromatic protons, repeating unit of PS), 5.97–5.77 (triazole-$CH_2N\mathbf{H}CO$), 4.61–4.33 [$OCH_2C\mathbf{H}_2$-triazole and $CH_2C\mathbf{H}$(Ph)-Br], 4.19–3.89 (triazole-$C\mathbf{H}_2NHCO$), 3.87–3.76 ($OC\mathbf{H}_2CH_2$-triazole), 3.74–3.48 ($C\mathbf{H}_2C\mathbf{H}_2O$, repeating unit of PEO), 3.38 ($C\mathbf{H}_3O$, end group of PEO), 2.58–1.16 [$C\mathbf{H}_2C\mathbf{H}$(Ph), repeating unit of PS backbone], 0.96–0.78 [NHCOC($C\mathbf{H}_3$)$_2$].

PEO-PS-N$_3$

PEO-PS-Br (1.50 g, 0.158 mmol, 1.0 equiv) and NaN_3 (0.21 g, 3.16 mmol, 20 equiv) were dissolved in 20 mL of dimethyl formamide (DMF). The reaction mixture was stirred for 17 h at room temperature. After removal of DMF using a rotary evaporator, the residue was redissolved in CH_2Cl_2. The solution was washed thrice with brine. After removal of the solvent, the crude product was purified thrice by dissolution/precipitation with CH_2Cl_2/methanol. The resulting polymer was dried at 30 °C in a vacuum oven for 24 h to give **PEO-PS-N$_3$** (1.13 g, 75%) as a white solid. $M_w/M_{n(GPC)} = 1.03$.

^1H NMR (500 MHz, $CDCl_3$): δ 7.51–7.43 (proton in triazole), 7.26–6.27 (aromatic protons, repeating unit of PS), 5.97–5.73 (triazole-$CH_2N\mathbf{H}CO$), 4.54–4.35 ($OCH_2C\mathbf{H}_2$-triazole), 4.21–3.87 [triazole-$C\mathbf{H}_2NHCO$ and $CH_2C\mathbf{H}$(Ph)-N_3], 3.87–3.76 ($OC\mathbf{H}_2CH_2$-triazole), 3.74–3.48 ($C\mathbf{H}_2C\mathbf{H}_2O$, repeating unit of PEO), 3.38 ($C\mathbf{H}_3O$, end group of PEO), 2.58–1.16 [$C\mathbf{H}_2C\mathbf{H}$(Ph), repeating unit of PS backbone], 0.98–0.75 [NHCOC($C\mathbf{H}_3$)$_2$].

(PEO-PS)$_2$-Acetylene

In a glove box, **PEO-PS-N$_3$** (0.88 g, 0.0926 mmol, 2.2 equiv), (3,5-bis(prop-2-ynyloxy)phenyl)methanol (**a**) (9.1 mg, 0.0421 mmol, 1.0 equiv), Cu(I)Br (242 mg, 1.68 mmol, 40 equiv), and deoxygenated PMDETA (291 mg, 1.68 mmol, 40 equiv) were dissolved in 10 mL of deoxygenated DMF. The reaction vessel was capped and removed from the glove box. The reaction mixture was then stirred for 10 h at room temperature. After removal of DMF using a rotary evaporator, the residue was redissolved in CH_2Cl_2. The organic solution was washed thrice with aqueous ethylenediaminetetraacetic acid solution. After removal of the solvent, the crude product was purified thrice by dissolution/precipitation with CH_2Cl_2/methanol. The resulting polymer was dried at 60 °C in a vacuum oven for 10 h to give a dimer with a hydroxyl end **(PEO-PS)$_2$-OH** (0.76 g, 95%) as a white solid. $M_w/M_{n(GPC)} = 1.06$.

^1H NMR (500 MHz, $CDCl_3$): δ 7.53–7.43 (protons in triazole), 7.26–6.27 (aromatic protons, repeating unit of PS), 5.97–5.79 (triazole-$CH_2N\mathbf{H}CO$), 5.18–4.92 [$CH_2C\mathbf{H}$(Ph)-triazole-$C\mathbf{H}_2O$], 4.58 ($C\mathbf{H}_2OH$), 4.54–4.35 ($OCH_2C\mathbf{H}_2$-triazole), 4.19–3.93 (triazole-$C\mathbf{H}_2NHCO$), 3.87–3.78 ($OC\mathbf{H}_2CH_2$-triazole), 3.74–3.48 ($C\mathbf{H}_2CH_2O$, repeating unit of PEO), 3.38 ($C\mathbf{H}_3O$), 2.58–1.16 [$C\mathbf{H}_2C\mathbf{H}$(Ph), repeating unit of PS backbone], 0.98–0.77 [NHCOC($C\mathbf{H}_3$)$_2$-PS].

The hydroxyl end was converted into an acetylene unit as follows: **(PEO-PS)$_2$-OH** (0.72 g, 0.0379 mmol, 1.0 equiv), dipentynoic anhydride (33.8 mg, 0.189 mmol, 5.0 equiv), DMAP (23.1 mg, 0.189 mmol, 5.0 equiv), and pyridine (30.0 mg, 0.379 mmol, 10 equiv) were dissolved in 10 mL of anhydrous CH_2Cl_2. The reaction mixture was stirred for 24 h at room temperature. After removal of the solvent, the crude product was purified six times by dissolution/precipitation with CH_2Cl_2/methanol. The collected polymer was then dried at 30 °C in a vacuum oven for 12 h to give **(PEO-PS)$_2$-acetylene** (0.50 g, 70%) as a white solid. $M_w/M_{n(GPC)} = 1.06$.

^1H NMR (500 MHz, $CDCl_3$): δ 7.55–7.42 (protons in triazole), 7.26–6.27 (aromatic protons, repeating unit of PS), 5.95–5.77 (triazole-$CH_2N\mathbf{H}CO$), 5.18–4.92 [PS-$CH_2C\mathbf{H}$(Ph)-triazole-$C\mathbf{H}_2O$ and $C\mathbf{H}_2OOCCH_2CH_2C{\equiv}CH$], 4.54–4.35 ($OCH_2C\mathbf{H}_2$-triazole), 4.19–3.93 (triazole-$C\mathbf{H}_2NHCO$), 3.87–3.78 ($OC\mathbf{H}_2CH_2$-triazole), 3.74–3.48 ($C\mathbf{H}_2C\mathbf{H}_2O$, repeating unit of PEO), 3.38 ($C\mathbf{H}_3O$), 2.58 ($C\mathbf{H}_2CH_2C{\equiv}CH$), 2.51 ($CH_2C\mathbf{H}_2C{\equiv}CH$), 2.42–1.16 [$C\mathbf{H}_2C\mathbf{H}$(Ph), repeating unit of PS backbone], 0.98–0.77 [NHCOC($C\mathbf{H}_3$)$_2$].

PLA-N$_3$

In a glove box, to a solution of tri(ethylene glycol) monoazide (175.6 mg, 1.0 mmol, 1.0 equiv) in anhydrous toluene

(100 mL), 1.0 M Et_3Al in hexane solution (0.5 mL, 0.5 mmol, 0.5 equiv) was added using a syringe at room temperature. The solution was stirred for 16 h, and D,L-lactide (13 g, 90 mmol, 90 equiv) was then added to the reaction mixture. The reaction vessel was placed in an oil bath at 90 °C for 3 h. After cooling to room temperature, the reaction was terminated with 1.0 M acidic methanol (7.0 mL, 7.0 mmol, 7.0 equiv). After pouring excess of methanol into the mixture solution, the resulting precipitate was purified several times by dissolution/precipitation with CH_2Cl_2/*n*-hexane. The collected solid was then dried at 40 °C in a vacuum oven for 10 h to yield **PLA-N$_3$** (7.1 g, 55%) as a white solid. M_w/M_n (GPC) $= 1.06$. $M_{n(NMR)} = 10{,}500$ g/mol.

^{1}H NMR (500 MHz, $CDCl_3$): δ 5.29–5.07 [br, 144H, OOCC**H**(CH_3), repeating unit of PLA], 4.36 [m, 1H, OOCC**H**(CH_3)OH, end group of PLA], 4.29 [m, 2H, $N_3CH_2CH_2OCH_2$-$CH_2OCH_2C\mathbf{H_2}OOCCH(CH_3)O$ of initiator], 3.74–3.61 [m, 8H, $N_3CH_2C\mathbf{H_2}OC\mathbf{H_2}C\mathbf{H_2}OC\mathbf{H_2}CH_2OOCCH(CH_3)O$ of initiator], 3.39 [t, 2H, $N_3C\mathbf{H_2}CH_2OCH_2CH_2OCH_2CH_2OOCCH(CH_3)O$ of initiator], 2.70 [d, 1H, —OOCCH(CH_3)O**H**, end group of PLA], 1.77–1.38 [br, 450H, —OOCCH(C**H$_3$**)O, repeating unit of PLA].

(PEO-PS)$_2$-PLA Terpolymer (1)

In a glove box, **(PEO-PS)$_2$-acetylene** (0.2 g, 0.0105 mmol, 1.0 equiv), **PLA-N$_3$** (0.221 g, 0.021 mmol, 2.0 equiv), Cu(I)Br (30.1 mg, 0.21 mmol, 20 equiv), and deoxygenated PMDETA (36.4 mg, 0.21 mmol, 20 equiv) were dissolved in 5 mL of deoxygenated anhydrous THF. The reaction vessel was capped and removed from the glove box. The reaction mixture was stirred for 24 h at room temperature. The reaction solution was then diluted with THF and passed through a neutral alumina column to remove the copper complex. The solvent was removed using a rotary evaporator, and the crude product was purified by flash silica-column chromatography (from CH_2Cl_2:EtOAc $= 1{:}1$ to CH_2Cl_2:methanol $= 8{:}1$) and preparative GPC. The obtained polymer was dried at 30 °C in a vacuum oven for 24 h to give the final polymer (**1**, 0.22 g, 70%) as a white solid. M_w/M_n (GPC) $= 1.10$.

^{1}H NMR (500 MHz, $CDCl_3$): δ 7.55–7.42 (protons in triazole), 7.26–6.27 (aromatic protons, repeating unit of PS), 5.95–5.77 (triazole-$CH_2N\mathbf{H}CO$), 5.30–5.10 [OOCC**H**(CH_3), repeating unit of PLA], 5.18–4.92 [PS-$CH_2C\mathbf{H}$(Ph)-triazole-$C\mathbf{H_2}$O and $C\mathbf{H_2}OOCCH_2CH_2$-triazole], 4.54–4.40 [PEO-$OCH_2C\mathbf{H_2}$-triazole and triazole-$C\mathbf{H_2}CH_2O(CH_2CH_2O)_2$-PLA], 4.37 [OOCC**H**($CH_3$)-OH, end group of PLA], 4.32–4.21 [triazole-$(CH_2CH_2O)_2CH_2$-$C\mathbf{H_2}$O-PLA], 4.19–3.93 (triazole-$C\mathbf{H_2}NHCO$), 3.87–3.78 (PEO-$OC\mathbf{H_2}CH_2$-triazole), 3.74–3.48 ($C\mathbf{H_2}C\mathbf{H_2}O$, repeating unit of PEO), 3.38 ($C\mathbf{H_3}O$), 3.10–2.96 ($CH_2OOCCH_2C\mathbf{H_2}$-triazole), 2.83–2.75 ($CH_2OOCC\mathbf{H_2}CH_2$-triazole), 2.75–2.65 [OOCH(CH_3)-O**H**], 2.42–1.16 [$C\mathbf{H_2}C\mathbf{H}$(Ph), repeating unit of PS backbone], 0.96–0.79 [NHCOC(C**H$_3$**)$_2$].

RESULTS AND DISCUSSION

The miktoarm terpolymer (**1**), (PEO-PS)$_2$-PLA, consists of three different blocks: PEO, PS, and PLA. The PEO with M_n of 2000 g/mol was commercially available, and the PS and PLA were synthesized by ATRP and ROP, respectively. As mentioned in the "Introduction" section, we used stepwise click reactions to combine the individually prepared polymeric blocks because of the high reactivity. The initiator (**acetylene-initiator**) for the ATRP and the A_2B-type branching precursor (**a**) were designed to contain acetylene units (Scheme 1). The amide linkage in the **acetylene-initiator** was chosen to be intact during the hydrolytic etching of the PLA block for the preparation of nanoporous materials. The click reactions in this study used Cu(I)Br/PMDETA and Cu(II) sulfate/sodium ascorbate as catalysts.

First, the PS block was synthesized by an ATRP using **acetylene-initiator** (Scheme 2). The ATRP of styrene was carried out using Cu(I)Br/PMDETA as the catalyst. In the ^{1}H NMR spectrum of the obtained PS (**acetylene-PS-Br**), the methylene group next to the acetylene unit was observed at 3.60 ppm, and the methine of the PS end appeared at 4.50 ppm [Fig. 1(a)]. The GPC data exhibited a narrow molecular weight distribution (M_w/M_n) of 1.04 [Fig. 2(a)]. The number–average molecular weight (M_n) from the GPC was determined to be 7800 g/mol, which was similar to the M_n (7500 g/mol) determined by the end-group analysis from the ^{1}H NMR. In the second step, the PS was coupled with the PEO block (**PEO-N$_3$**) with an azide end (M_n of the PEO: 2000 g/mol) using the click reaction. In this click reaction, a small excess of the PS precursor (**acetylene-PS-Br**) was used. The remaining PS was readily removed from the product (**PEO-PS-Br**) using a column chromatography because of the considerable polarity difference. In the ^{1}H NMR, the product exhibited a proton of the formed 1,2,3-triazole near 7.50 ppm [Fig. 1(b)]. In the GPC data, the product, despite its larger size, eluted slower than **acetylene-PS-Br** [Fig. 2(b)]. This behavior was due to the interaction between PEO chains and GPC column.[14]

To perform the next click coupling with the branching precursor (**a**), the bromide end of the PS block (**PEO-PS-Br**) was converted into an azide group using sodium azide in DMF. This reaction was quantitative, and therefore, it has frequently been used to prepare PS precursors for click chemistry.[15] The obtained PEO-PS diblock copolymer (**PEO-PS-N$_3$**) was dimerized by the second click reaction with the branching precursor (**a**) bearing two acetylene units and a hydroxyl group. After the completion of the dimerization reaction, a tiny amount of leftover **PEO-PS-N$_3$** was removed by several dissolution/precipitation cycles with CH_2Cl_2/methanol. Subsequently, an acetylene unit was attached by the esterification of the focal hydroxyl group and dipentynoic anhydride. The obtained compound, **(PEO-PS)$_2$-acetylene**, was consistent with the expected molecular structure. The ^{1}H NMR data displayed two methylene signals of the pentynoic group near 2.50 ppm [Fig. 1(d)]. The GPC data showed a molecular weight distribution of 1.06 [Fig. 2(c)].

Meanwhile, the ROP of D,L-lactide was performed using triethyl aluminum as the catalyst, as described previously.[13] In this case, tri(ethylene glycol) monoazide was used as the initiator because of the final click coupling with **(PEO-PS)$_2$-acetylene**. The molecular weight of the resulting PLA

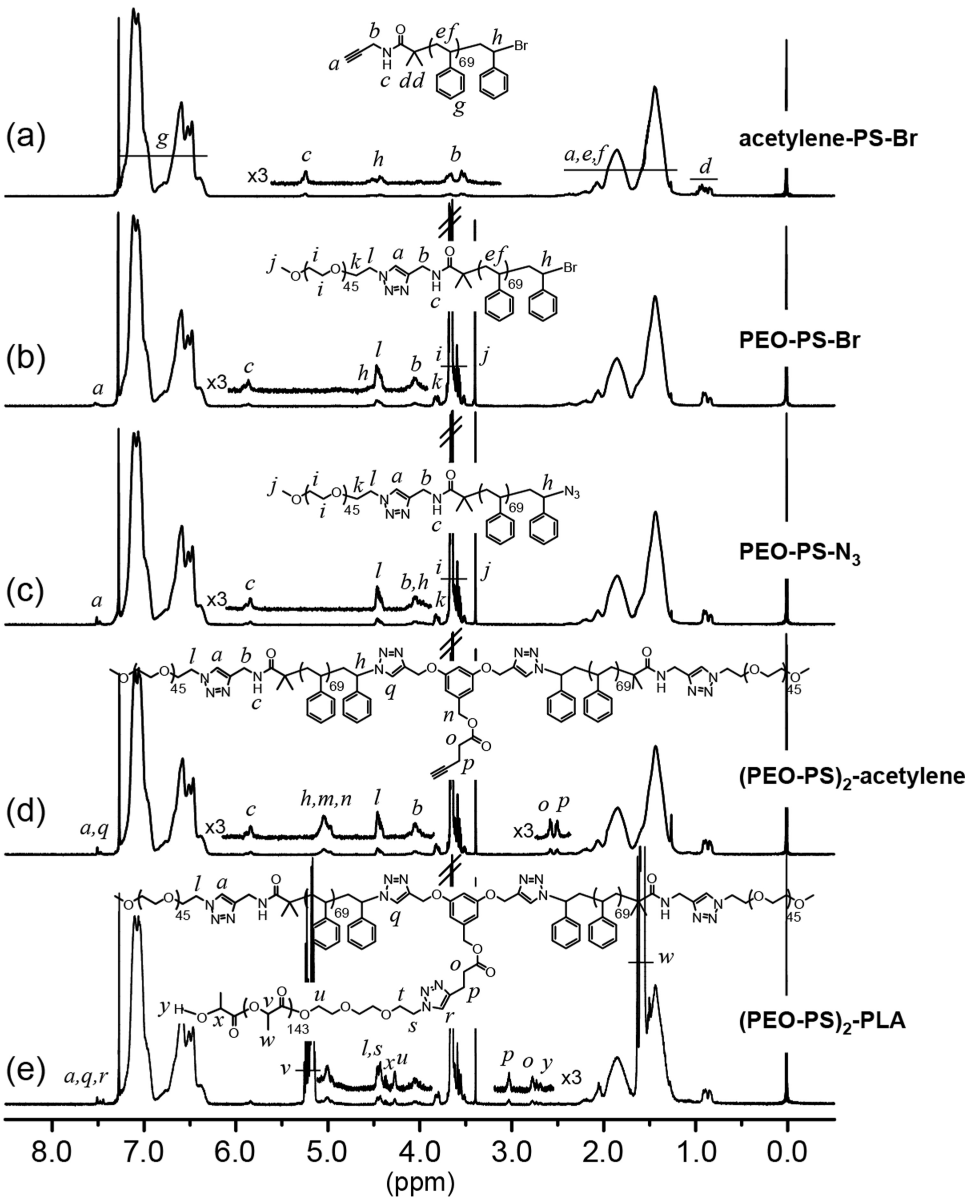

FIGURE 1 ^{1}H NMR spectra of (a–d) intermediate compounds and (e) terpolymer (**1**).

(**PLA-N$_3$**) was determined as 10,500 g/mol from the ^{1}H NMR data, and the molecular weight distribution was 1.06 from the GPC elugram [Fig. 2(d)].

The final click reaction of **(PEO-PS)$_2$-acetylene** and **PLA-N$_3$** produced the miktoarm (PEO-PS)$_2$-PLA terpolymer (**1**). In this reaction, an excess of the PLA block was used. The PLA block moved by a column chromatography using dichloromethane:ethyl acetate = 1:1 as the eluent, whereas the terpolymer did not move at all. Therefore, the PLA precursor could be simply isolated, and the product was then collected using more polar mixture eluent such as CH_2Cl_2:methanol = 8:1. After the column chromatography, a preparative GPC purification was further performed for the complete isolation. The final product was characterized by ^{1}H NMR, GPC, and MALDI-TOF mass techniques. The ^{1}H NMR spectrum of the isolated terpolymer showed PS, PLA, and PEO regions, and linkage protons could be observed at the expected positions [Fig. 1(e)]. The molecular weight distribution of the final terpolymer was 1.10 in the GPC data [Fig. 2(e)]. In addition, the mass spectrum exhibited the signal center near 28,000 g/mol, which is analogous to the theoretical molecular weight of 29,500 g/mol calculated from the ^{1}H NMR data [Fig. 2(f)].

Thermal and Self-Assembling Behavior of the Terpolymer and Its Ionic Sample

In this study, one of our interests was the influence of the ion doping in the PEO block on the self-assembling behavior of the miktoarm terpolymer. To do this, we compared the thermal and self-assembling behavior of pristine terpolymer (**1**) and its ion-doped sample (**1-Li$^+$**). The terpolymer was ion doped using lithium triflate, whose concentration per ethylene oxide was chosen to be 0.2.

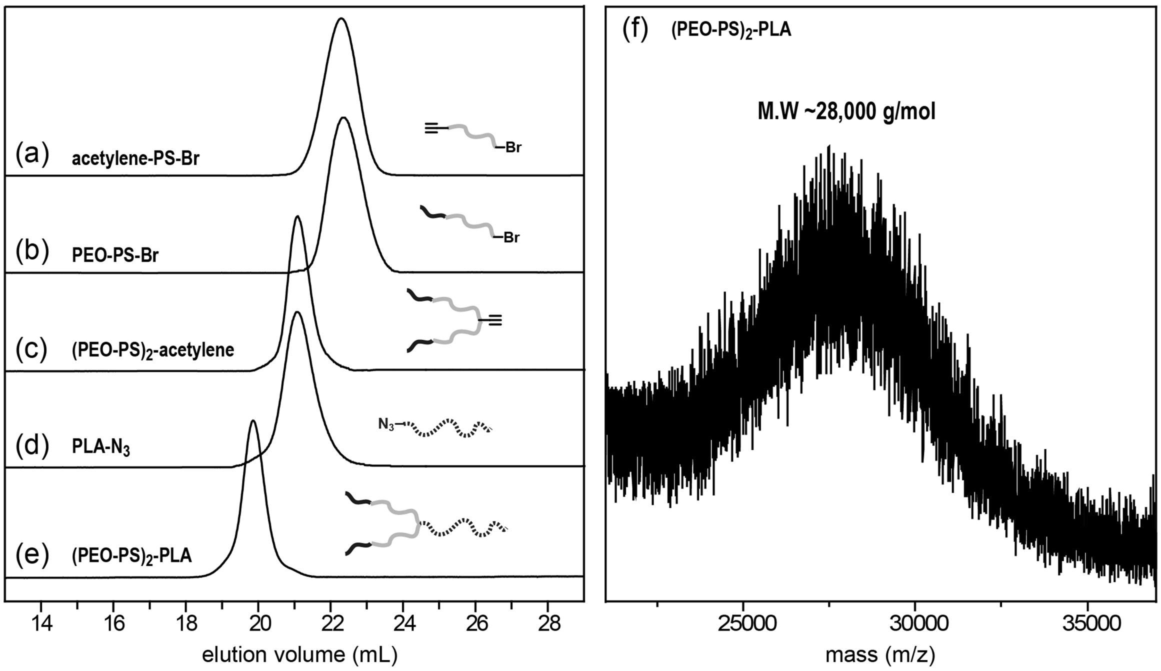

FIGURE 2 (a–e) GPC traces of polymers and (f) MALDI-TOF mass spectrum of the $(PEO-PS)_2$-PLA terpolymer.

Microphase separation between the blocks could be investigated by examining the thermal properties such as melting and glass transition temperatures (T_m and T_g). The thermal behavior of **1** and **1-Li**$^+$ were examined by DSC. No observation of any significant melting transition in the DSC data of **1** indicates the absence of PEO crystallization, which may support the mixing of the PEO and PLA blocks. Before adding lithium salt, the terpolymer displayed two glass transitions at 18.6 and 61.7 °C [Fig. 3(a)]. These transitions probably correspond to the glass transitions of PEO/PLA domain and PS, respectively, because PEO block is more compatible with PLA than PS. Assuming that PEO and PLA blocks were mixed, the T_g calculation using the Fox equation gave the transition at 19.7 °C.[16] This strongly suggests that the T_g at 18.6 °C is attributed to the PEO/PLA domains, which are separated from PS. The T_g of the PS block in this terpolymer was estimated to be lower than linear PS with similar molecular weights.[17] This might be due to the fact that the PS block is connected at three junction points with PEO and PLA chains, and thus it is partially mixed with the other blocks (particularly PEO, because PS is more compatible with PEO than PLA). Based on the DSC results, it could be considered that a microstructure assembled from the

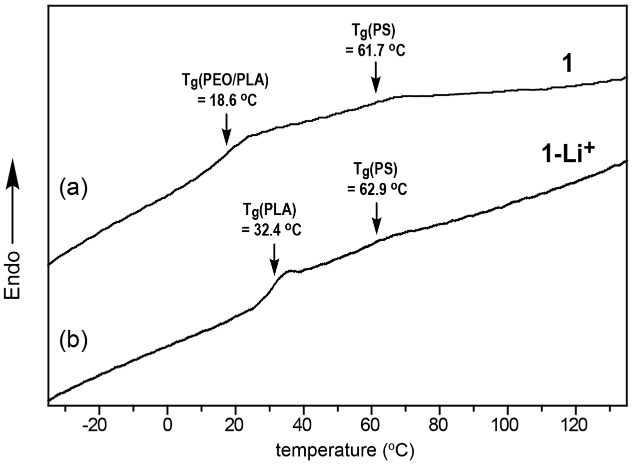

FIGURE 3 DSC thermograms of (a) **1** and (b) 1-Li$^+$.

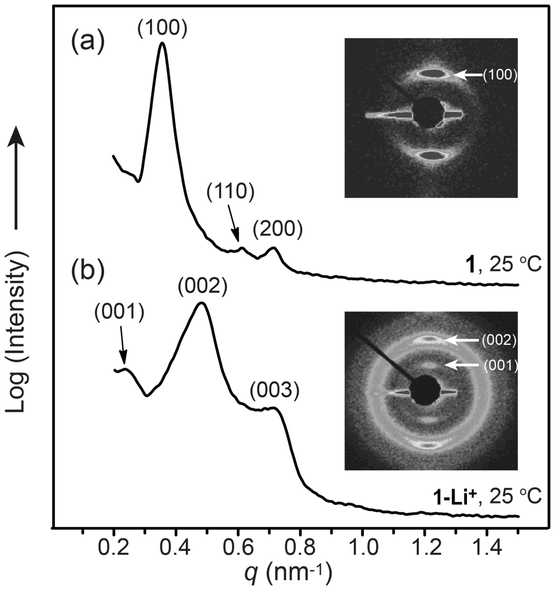

FIGURE 4 SAXS data of (a) 1 and (b) 1-Li$^+$. The two-dimensional SAXS data were obtained from the aligned samples using a channel die.

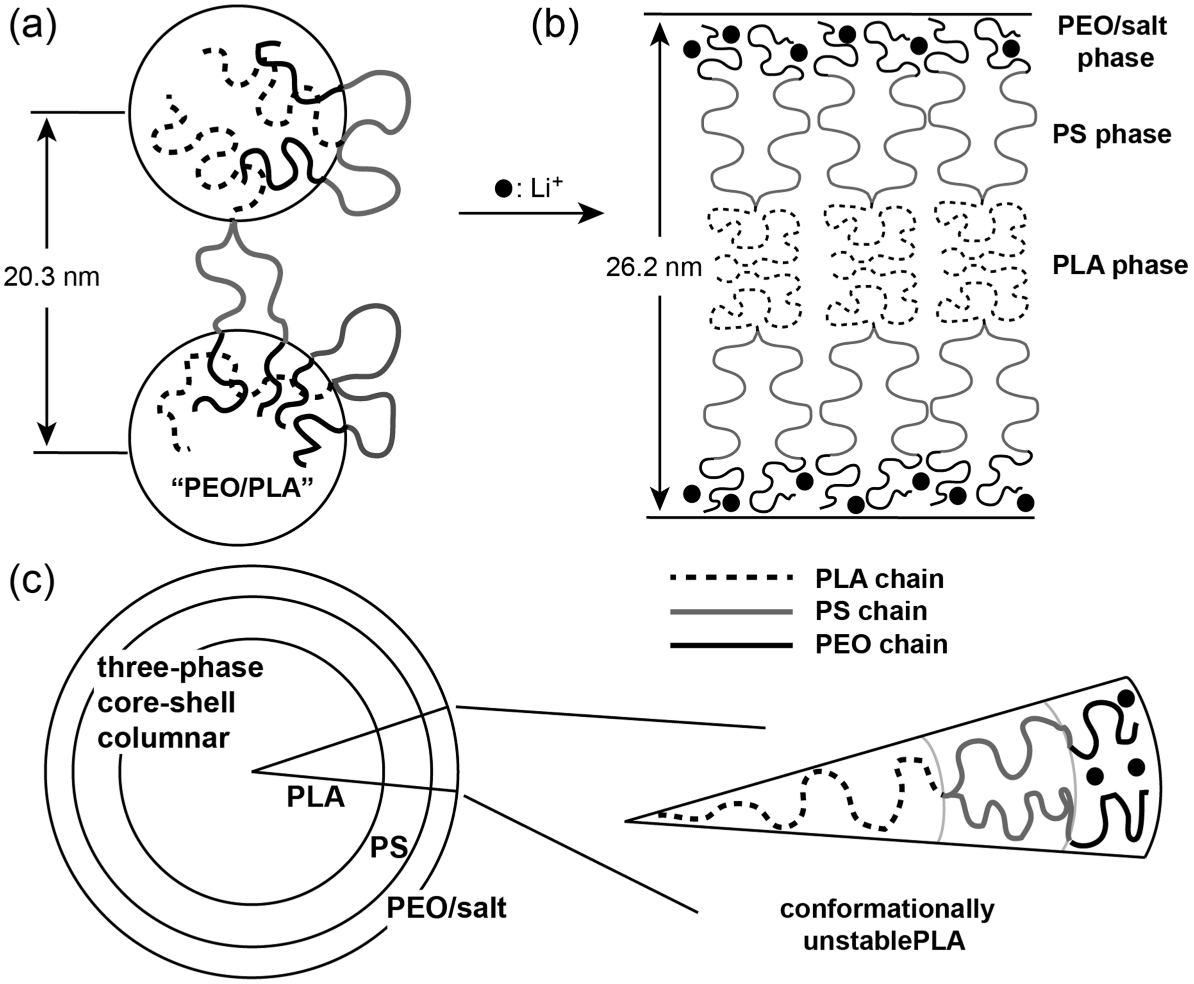

FIGURE 5 Transformation from (a) two-phase columnar to (b) three-phase lamellar morphologies on doping lithium salt and (c) stretched PLA chain in the core region of a unfavorable three-phase columnar structure.

terpolymer would consist of two segregated domains such as PS and PEO/PLA regions.

On the other hand, on doping lithium salt, two T_gs were observed at 32.4 and 62.9 °C [Fig. 3(b)]. The higher glass transition was almost identical to the T_g of the PS before ion doping, whereas the lower glass transition increased by 14 °C, in comparison with the T_g of the PEO/PLA region before ion doping. This suggests that a microphase separation between the PEO and PLA blocks occurred on ion doping. Thus, the observed lower T_g could correspond to the PLA-rich domain. No noticeable T_g for the PEO–lithium salt was observed in this DSC experiment, which might be due to the relatively small weight fraction (0.13) of the PEO block.

The assembled microstructures of **1** and **1-Li**$^+$ were characterized by temperature-variable SAXS experiments. Both samples displayed ordered morphologies up to 200 °C, which was the experimentally accessible temperature. The SAXS data of the miktoarm terpolymer (**1**) showed three reflections with q-spacing ratios of 1:v3:v4, which correspond to the (100), (110), and (200) planes of a hexagonal columnar structure [Fig. 4(a)]. From the observed primary peak, the intercolumnar distance was estimated to be 20.3 nm. Considering the volume fraction ($f = 0.54$) of the PS block and the above DSC analysis, the hexagonal columnar structure consists of PEO/PLA cylindrical domains surrounded by PS blocks [Fig. 5(a)].

In contrast, **1-Li**$^+$ exhibited a considerably distinct SAXS pattern from **1**. The SAXS data at 25 °C displayed three reflections with q-spacing ratios of 1:2:3, suggestive of a lamellar structure [Fig. 4(b)]. More obviously, three reflections could be recognized in the two-dimensional SAXS data of a macroscopically aligned sample. The notable feature in this SAXS pattern was the relative intensity of the reflections. In general, the relative intensity depends not only on the volume fraction but also on the electron density of each block. In contrast to the conventional two-phase lamellar structures, in this case, the second peak is the most intense instead of the first peak. This unusual pattern has been observed in several three-phase lamellar structures.[18] Therefore, the SAXS pattern suggests that microphase separation between PEO and PLA blocks occurred on lithium doping, leading to a three-phase lamellar structure [Fig. 4(b)]. From the (001)

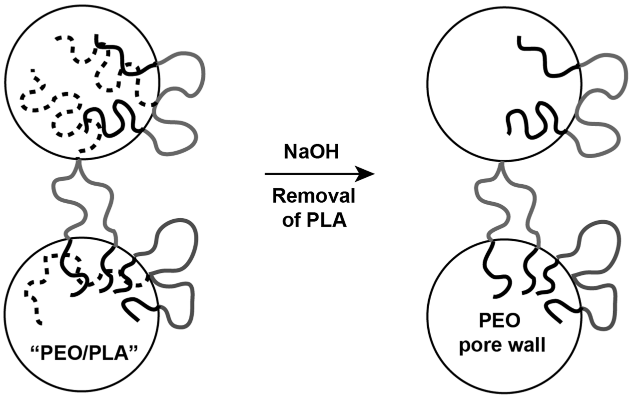

FIGURE 6 Preparation of **Porous PS-PEO** by a hydrolytic etching of the PLA block of the terpolymer (**1**).

peak, the periodic lamellar thickness was estimated to be 26.2 nm.

One may consider the formation of three-phase core–shell columnar structure with a curved interface on ion doping [Fig. 5(c)]. However, the three-phase lamellar structure might be thermodynamically more stable in terms of the conformational energy of the longest PLA chain. Assuming that **1-Li**$^+$ forms a core–shell columnar structure, the PLA block will be located in the cylindrical core region. The branched and short PEO blocks cannot pack the cylindrical core efficiently; however, if packed, a large steric hindrance associated with the branches will take place at the PS/PEO interface. Therefore, in the core–shell columnar morphology, the linear PLA chain will occupy the cylindrical core due to the dendritic chain architecture, although it is the longest chain [Fig. 5(c)]. However, the PLA will be conformationally destabilized by the stretching penalty in the narrow cylindrical core.[3(a),19] On the other hand, the three-domain lamellar structure is more favorable with respect to the PLA conformation. The lamellar formation can provide a less anisotropic space for the PLA at the expense of the conformational entropies of shorter PS and PEO chains, because the PLA conformation stabilization is more dominant than those of the shorter blocks [Fig. 5(b)]. Consequently, the transformation from the two-phase columnar to three-phase lamellar structure on lithium doping can be explained by (i) microphase separation between PEO and PLA blocks and (ii) the alleviation of the conformational energy of the longest PLA chain.

Preparation of Nanoporous PS-PEO by the Chemical Etching of the Terpolymer

As mentioned previously, the structural interpretation of terpolymer **1** suggested that the PS block occupies the continuous matrix of the hexagonal columnar structure, whereas the PEO and PLA blocks are mixed in the confined core region (Fig. 5). It is well known that the PLA block can be hydrolytically degraded, whereas the PS and PEO blocks are intact in the presence of NaOH, and the PS block is mechanically robust below its T_g of 61.7 °C. Therefore, we considered that a chemical etching using NaOH would produce a nanoporous PS-PEO with a regular array of nanopores (Fig. 6). Hairy PEO chains remaining after the chemical etching would make the pore wall hydrophilic. With this in mind, we attempted to prepare a porous PS-PEO (**Porous PS-PEO**) using terpolymer **1**. For the thorough removal of the chemically cleavable PLA block, terpolymer **1** was macroscopically oriented using a channel die method. Otherwise, etchants would be hindered from accessing internal domains. The aligned sample was monolithic in nature. When the X-ray beam was perpendicular to the cylinder axes, two intense spots were observed in the two-dimensional SAXS data. This indicates a macroscopic orientation [Fig. 4(a)]. The PLA block of the monolithic sample could be hydrolytically degraded in 0.5 M NaOH solution (methanol:water = 2:3 vol %). The degradation temperature was set at 45 °C, which is lower than the T_g (61.7 °C) of the PS block [Fig. 3(a)]. The complete degradation of the PLA block was identified by the ^{1}H NMR spectrum, in which the methine protons of the PLA at 5.1–5.2 ppm disappeared after the chemical etching [Fig. 7(a)].

The monolithic nature was still observed in the etched porous sample (**Porous PS-PEO**). Like the sample before etching, two intense spots appeared in the two-dimensional SAXS data [Fig. 7(b)]. The presence of nanochannels was clearly validated by SEM. The side-view image displayed regularly arrayed furrows, and the top-view image showed hexagonally arranged nanopores (Fig. 8). The average pore diameter from the SEM images was about 10.0 nm. However, considering the thickness of the Pt coating (ca. 2.0 nm), the actual pore diameter could be assumed to be 14.0 nm.

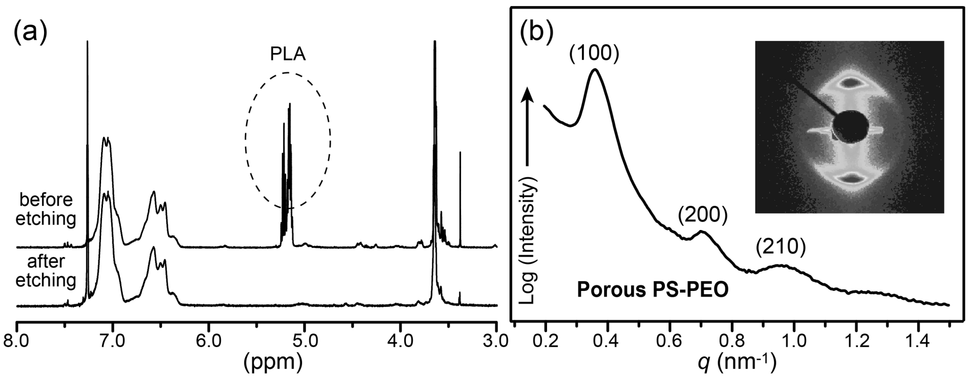

FIGURE 7 (a) ^{1}H NMR spectra before and after etching and (b) SAXS data of the porous sample (**Porous PS-PEO**) after etching.

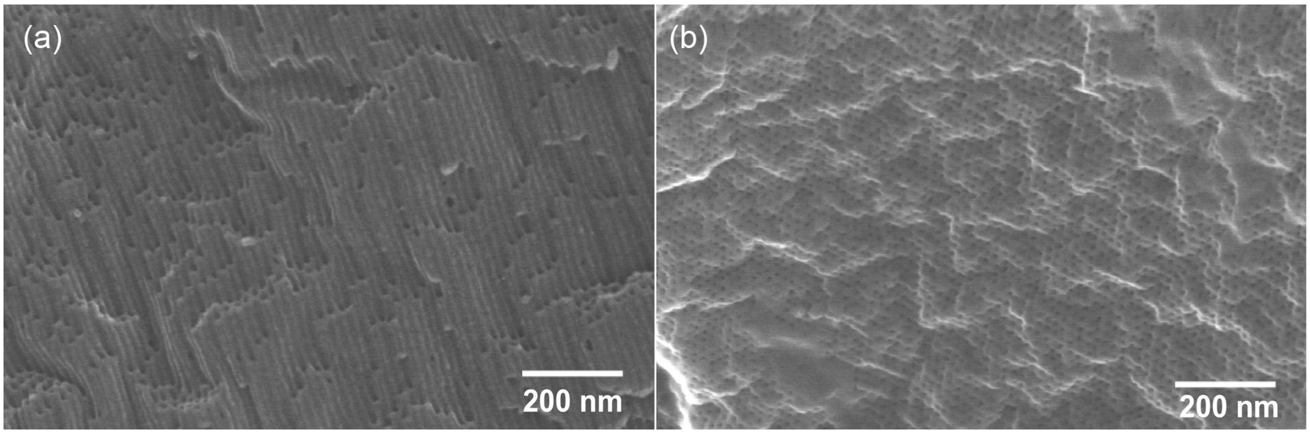

FIGURE 8 Scanning electron micrographs of **Porous PS-PEO**: (a) parallel and (b) perpendicular to the cylinder axes.

Several porous PS materials having sparse hydroxyl groups on the walls were known to be floating on the water because the whole wall properties were not hydrophilic enough for water uptake.[20] In contrast, **Porous PS-PEO** could sink to the bottom in water. This behavior must be due to enhanced water wettability of the pore wall composed of hydrophilic PEO chains.[21]

CONCLUSIONS

A dendritic terpolymer was successfully prepared via stepwise click reactions of individually prepared PEO, PS (by an ATRP), and PLA (by a ROP) blocks. The terpolymer self-assembled into a hexagonal columnar morphology consisting of PEO/PLA cylindrical cores and a PS matrix while a three-phase lamellar morphology was induced on doping lithium salt. This morphological transformation could be explained by (i) microphase separation between PEO and PLA blocks and (ii) alleviation of the conformational energy of the longest PLA chain. A nanoporous PS-PEO could be obtained by chemically etching the hexagonal columnar terpolymer using NaOH. The presence of PEO chain on the wall rendered the porous PS-PEO to be water compatible. The nanoporous material prepared via the terpolymer assembly could be used as a chromatographic substance for various nanosized analytes.

REFERENCES AND NOTES

1 Bosman, A. W.; Janssen, H. M.; Meijer, E. W. *Chem. Rev.* **1999,** *99*, 1665–1688.

2 (a) Rosen, B.; Wilson, C. J.; Wilson, D. A.; Peterca, M.; Imam, M. R.; Percec, V. *Chem. Rev.* **2009,** *109*, 6275–6540; (b) Khanna, K.; Varshney, S.; Kakkar, A. *Polym. Chem.* **2010,** *1*, 1171–1185; (c) Cho, B.-K.; Jain, A.; Gruner, S. M.; Wiesner, U. *Science* **2004,** *305*, 1598–1601; (d) Rangou, S.; Avgeropoulos, A. *J. Polym. Sci. Part A: Polym. Chem.* **2009,** *47*, 1567–1574; (e) Johnson, M. A.; Iyer, J.; Hammond, P. T. *Macromolecules* **2004,** *37*, 2490–2501; (f) Román, C.; Fischer, H. R.; Meijer, E. W. *Macromolecules* **1999,** *32*, 5525–5531; (g) Leduc, M. R.; Hawker, C. J.; Dao, J.; Fréchet, J. M. J. *J. Am. Chem. Soc.* **1996,** *118*, 11111–11118; (h) Percec, V.; Johansson, G.; Heck, J.; Ungar, G.; Batty, S. V. *J. Chem. Soc. Perkin Trans 1* **1993,** 1411–1420; (i) Percec, V.; Heck, J.; Tomazos, D.; Falkenberg, F.; Blackwell, H.; Ungar, G. *J. Chem. Soc. Perkin Trans. 1* **1993,** 2799–2811; (j) Percec, V.; Heck, J. A.; Tomazos, D.; Ungar, G. *J. Chem. Soc. Perkin Trans. 2* **1993,** 2381–2388; (k) Percec, V.; Topmazos, D.; Heck, J.; Blackwell, H.; Ungar, G. *J. Chem. Soc. Perkin Trans. 2* **1994,** 31–44; (l) Johansson, G.; Percec, V.; Ungar, G.; Abramic, D. *J. Chem. Soc. Perkin Trans. 1* **1994,** 447–459; (m) Percec, V.; Heck, J.; Johansson, G.; Tomazos, D.; Kawasumi, M.; Ungar, G. *J. Macromol. Sci. Pure Appl. Chem.* **1994,** *31*, 1031–1070; (n) Percec, V.; Heck, J.; Johansson, G.; Tomazos, D.; Ungar, G. *Macromol. Symp.* **1994,** *77*, 237–265; (o) Percec, V.; Heck, J.; Johansson, G.; Tomazos, D.; Kawasumi, M.; Chu, P.; Ungar, G. *J. Macromol. Sci. Pure Appl. Chem.* **1994,** *31*, 1719–1758.

3 (a) Chung, Y.-W.; Lee, J.-K.; Zin, W.-C.; Cho, B.-K. *J. Am. Chem. Soc.* **2008,** *130*, 7139–7147; (b) Lee, E.; Lee, B.-I.; Kim, S.-H.; Lee, J.-K.; Zin, W.-C.; Cho, B.-K. *Macromolecules* **2009,** *42*, 4134–4140; (c) Choi, J.-W.; Cho, B.-K. *J. Polym. Sci. Part A: Polym. Chem.* **2011,** *49*, 2468–2473.

4 (a) Liu, H.; Li, C.; Liu, H.; Liu, S. *Langmuir* **2009,** *25*, 4724–4734; (b) Li, C.; Ge, Z.; Liu, H.; Liu, S. *J. Polym. Sci. Part A: Polym. Chem.* **2009,** *47*, 4001–4013; (c) Erdogan, T.; Gungor, E.; Durmaz, H.; Hizal, G.; Tunca, U. *J. Polym. Sci. Part A: Polym. Chem.* **2006,** *44*, 1396–1403; (d) Liu, C.; Hillmyer, M. A.; Lodge, T. P. *Langmuir* **2008,** *24*, 12001–12009.

5 (a) Percec, V.; Barboiu, B.; Grigoras, C.; Bera, T. K. *J. Am. Chem. Soc.* **2003,** *125*, 6503–6516; (b) Percec, V.; Grigoras, C.; Kim, H.-J. *J. Polym. Sci. Part A: Polym. Chem.* **2004,** *42*, 505–513; (c) Percec, V.; Grigoras, C.; Bera, T. K.; Barboiu, B.; Bissel, P. *J. Polym. Sci. Part A: Polym. Chem.* **2005,** *43*, 4894–4906; (d) Rosen, B. M.; Percec, V. *Chem. Rev.* **2009,** *109*, 5069–5119.

6 (a) Rostovtsev, V. V.; Green, L. G.; Fokin, V. V.; Sharpless, K. B. *Angew. Chem. Int. Ed. Engl.* **2002,** *41*, 2596–2599; (b) Franc, G.; Kakkar, A. *Chem. Commun.* **2008,** 5267–5276; (c) Rosen, B. M.; Lligadas, G.; Hahn, C.; Percec, V. *J. Polym. Sci. Part A: Polym. Chem.* **2009,** *47*, 3940–3948; (d) Rosen, B. M.; Lligadas, G.; Hahn, C.; Percec, V. *J. Polym. Sci. Part A: Polym. Chem.* **2009,** *47*, 3931–3939; (e) Tasdelen, M. A. *Polym. Chem.* **2011,** *2*, 2133–2145.

7 (a) Ryu, M.-H.; Choi, J.-W.; Cho, B.-K. *J. Mater. Chem.* **2010,** *20*, 1806–1810; (b) Ryu, M.-H.; Choi, J.-W.; Kim, H.-J.; Park, N.; Cho, B.-K. *Angew. Chem. Int. Ed. Engl.* **2011,** *50*, 5737–5740; (c) Choi, J.-W.; Ryu, M.-H.; Lee, E.; Cho, B.-K. *Chem. Eur. J.* **2010,** *16*, 9006–9009; (d) Choi, J.-W.; Cho, B.-K. *Soft Matter* **2011,** *7*, 4045–4049; (e) Xia, Y.; Verduzco, R.; Grubbs, R. H.; Kornfield, J. A. *J. Am. Chem. Soc.* **2008,** *130*, 1735–1740; (f) Gallardo, H.; Ely, F.; Bortoluzzi, A. J.; Conte.G. *Liq. Cryst.* **2005,** *32*, 667–671.

8 Hadjichristidis, N.; Iatrou, H.; Pitsikalis, M.; Mays, J. *Prog. Polym. Sci.* **2006,** *31*, 1068–1132.

9 Younes, H.; Cohn, D. *Eur. Polym. J.* **1988,** *24*, 765–773.

10 (a) Kim, H.-Y.; Song, J.; Kim, S.-H.; Lee, E.; Lee, J.-K.; Zin, W.-C.; Cho, B.-K. *Chem. Eur. J.* **2009,** *15*, 8683–8686; (b) Cho, B.-K.; Kim, S.-H.; Lee, E. *J. Polym. Sci. Part A: Polym. Chem.* **2010,** *48*, 2372–2376; (c) Cai, H.; Jiang, G.; Shen, Z.; Fan, X. *Macromolecules* **2012,** *45*, 6176–6184.

11 (a) Olson, D. A.; Chen, L.; Hillmyer, M. A. *Chem. Mater.* **2008,** *20*, 869–890; (b) Ho, R.-M.; Chen, C.-K.; Chiang, Y.-W.; Ko, B.-T.; Lin, C.-C. *Adv. Mater.* **2006,** *18*, 2355–2358.

12 Altintas, O.; Hizal, G.; Tunca, U. *J. Polym. Sci. Part A: Polym. Chem.* **2006,** *44*, 5699–5707.

13 Ha, J.-G.; Song, J.; Lee, J.-K.; Cho, B.-K.; Zin, W.-C. *Chem. Commun.* **2012,** *48*, 3418–3420.

14 Huang, K.; Rzayev, J. *J. Am. Chem. Soc.* **2009,** *131*, 6880–6885.

15 (a) Golas, P. L.; Matyjaszewski, K. *QSAR Comb. Sci.* **2007,** *26*, 1116–1134; (b) Wang, K.; Liang, L.; Lin, S.; He, X. *Eur. Polym. J.* **2008,** *44*, 3370–3376.

16 Mao, H.; Hillmyer, M. A. *Macromol. Chem. Phys.* **2008,** *209*, 1647–1656.

17 Song, J.; Cho, B.-K. *Bull. Korean Chem. Soc.* **2008,** *29*, 1167–1172.

18 (a) Bailey, T. S.; Pham, H. D.; Bates, F. S. *Macromolecules* **2001,** *34*, 6994–7008; (b) Kang, Y.-S.; Zin, W.-C.; Lee, D.-W.; Lee, M. *Liq. Cryst.* **2000,** *27*, 1543–1550.

19 Frischknecht, A.; Fredrickson, G. H. *Macromolecules* **1999,** *32*, 6831–6836.

20 (a) Zalusky, A. S.; Olayo-Valles, R.; Taylor, C. J.; Hillmyer, M. A. *J. Am. Chem. Soc.* **2001,** *123*, 1519–1520; (b) Zalusky, A. S.; Olayo-Valles, R.; Wolf, J. H.; Hillmyer, M. A. *J. Am. Chem. Soc.* **2002,** *124*, 12761–12773; (c) Mao, H.; Hillmyer, M. A. *Soft Matter* **2006,** *2*, 57–59.

21 (a) Rzayev, J.; Hillmyer, M. A. *Macromolecules* **2005,** *38*, 3–5; (b) Bailey, T. S.; Rzayev, J.; Hillmyer, M. A. *Macromolecules* **2006,** *39*, 8772–8781; (c) Mao, H.; Arrechea, P. L.; Bailey, T. S.; Johnson, B. J. S.; Hillmyer, M. A. *Faraday Discuss.* **2005,** *128*, 149–162.